Microchemical Journal 204 (2024) 111132

Contents lists available at ScienceDirect

Microchemical Journal

journal homepage: www.elsevier.com/locate/microc

A luminescent metal–organic framework composite as a turn-on sensor for the selective determination of monosodium glutamate in instant noodles

Alaa Bedair [a], Reda M. Abdelhameed [b], Sherin F. Hammad [c], Inas A. Abdallah [a], Marcello Locatelli [d,*], Fotouh R. Mansour [c,*]

[a] Department of Analytical Chemistry, Faculty of Pharmacy, University of Sadat City, Sadat City, 32897, Monufia, Egypt
[b] Applied Organic Chemistry Department, Chemical Industries Research Institute, National Research Centre, Giza 12622, Egypt
[c] Department of Pharmaceutical Analytical Chemistry, Faculty of Pharmacy, Tanta University, Tanta, 31111, Egypt
[d] Department of Pharmacy, University "G. d'Annunzio" of Chieti-Pescara, Via dei Vestini 31, 66100 Chieti, Italy

ARTICLE INFO

Keywords:
Metal organic framework
Fluorescence
Sensor
Monosodium glutamate
Microcrystalline cellulose
Instant noodles

ABSTRACT

This work reports the development and application of a new fluorescent nanoprobe sensor depending on using luminescent metal organic framework (LMOF). The developed sensor composed of hybridized Ca 1,3,5-benzene-tricarboxylic acid metal organic framework with microcrystalline cellulose (Ca-BTC/MCC MOF) as a fluorescent probe for the determination of the monosodium glutamate (MSG), a non-chromophoric food additive. The developed sensor was characterized using a high-resolution scanning electron microscope (HR-SEM), X-ray diffraction (XRD), and Fourier transform infrared spectroscopy (FTIR). The Ca-BTC/MCC MOF hybrid, examined under the HR-SEM, showed morphological features different from the MCC and the Ca-BTC MOF. The diffraction patterns of Ca-BTC/MCC composites clearly displayed the characteristic Ca-BTC MOF diffraction bands, indicating that MCC was successfully incorporated in the formation of crystalline MOF hybrids. The FTIR spectra show the bands of MCC, as well as the bands of Ca-BTC MOFs. The prepared nanoprobe was successfully applied as a sensitive sensor for the determination of MSG in food sample. The method was validated following the International ICH (Q2)R2 guidelines in terms of precision, trueness and other main analytical figures of merit, comprised the green profile and practicability metrics. A wide linearity range was achieved (5–50 μg/mL) with good correlation coefficient ($R^2 \geq 0.9993$). The recoveries (%) were found in the range of 100.0 to 101.5 and the RSDs (%) were in the range of 0.1 to 0.9 %.

These results show that the developed nanoprobe was selective, and highly accurate to determine this important food additive in the seasonings of instant noodles, also showing a reduced environmental impact based on the metrics currently accepted for the evaluation of the green profile and practicability.

1. Introduction

Monosodium glutamate (MSG, E621) is a common food additive with a distinct Umami flavor [1,2]. This widely used additive is the sodium salt of glutamate, a non-essential amino acid with the chemical name 2-aminopentanedioic acid [3,4]. MSG is commonly used as a flavor enhancer in a variety of foods and medications [5]. The reasonable consumption of MSG was assessed by the Food and Drug Administration (FDA) to be roughly 0.55 g/day, with a maximum limit of 1.0 g/day [6]. This threshold is related to the fact that glutamate is an effective excitatory neurotransmitter in the human brain. Excessive MSG consumption could causes neurological illnesses such as Parkinson's and Alzheimer's diseases [7]. Glutamate may accumulate and become harmful if the glutamate receptor inactivation is not balanced by glutamate absorption in the synaptic cleft [8]. Accordingly, memory, learning, and regulatory processes are all affected by excessive MSG intake. According to the Federation of American Societies for Experimental Biology (FASEB), high-dose MSG exposure can cause a transient MSG disorder known as Chinese restaurant syndrome [9], manifested as flushing, headache, numbness in the mouth, and other symptoms such as burning sensations, facial pressure, and chest pains [6]. Furthermore, high MSG consumption is linked to diabetes and obesity. For these

* Corresponding authors at: Department of Pharmaceutical Analytical Chemistry, Faculty of Pharmacy, Elgeish Street, the medical campus of Tanta University, Tanta 31111, Egypt (F.R. Mansour). Department of Pharmacy, University "G. d'Annunzio" of Chieti-Pescara, Via dei Vestini 31, 66100 Chieti, Italy (M. Locatelli).
E-mail addresses: marcello.locatelli@unich.it (M. Locatelli), fotouhrashed@pharm.tanta.edu.eg (F.R. Mansour).

https://doi.org/10.1016/j.microc.2024.111132
Received 27 May 2024; Received in revised form 1 July 2024; Accepted 4 July 2024
Available online 5 July 2024

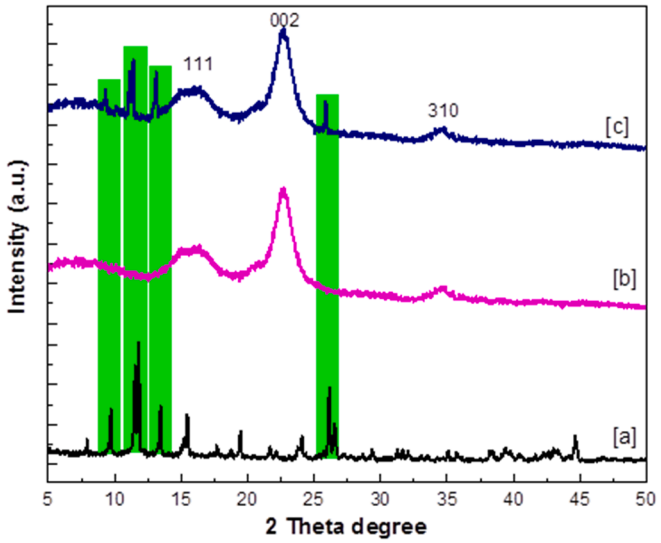

Fig. 1. Infrared spectra of [a] the MCC polymer, [b] the Ca-BTC MOF, and [c] the Ca-BTC/MCC hybrid.

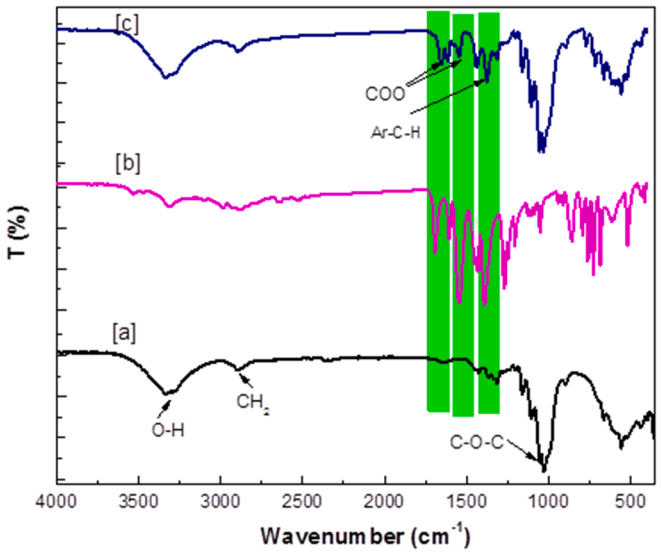

Fig. 2. X-ray diffraction pattern of the MCC polymer, [b] the Ca-BTC MOF, and [c] the Ca-BTC/MCC MOF hybrid.

reasons, routine determination of MSG in food stuff is critical [10].

Several methods for the determination of MSG have been developed, including UV/Visible spectrophotometry [7,11–15], spectrofluorimetry [16–18], paper and thin layer chromatography [19], High Performance Liquid Chromatography (HPLC) combined with different detectors [20–22], electrochemistry [9,23,24] and capillary electrophoresis [25]. The spectroscopic determination of MSG is challenging because it is a non-aromatic amino acid with no extended conjugation or strong chromophoric groups, which hinders its direct detection by spectrophotometric or spectrofluorometric methods. Alternatively, MSG is commonly determined by employing selective enzymatic processes, chemical derivatization of the aliphatic amino group, or inserting the amino acid into a complex formation reaction that results in the synthesis of colored or luminous compounds. However, these procedures need the use of costly chemicals, extensive reaction times, heating, or catalysis, making MSG determination hard, time-consuming and expensive [26].

Metal-organic frameworks (MOFs) are a novel class of sensing materials that have emerged in the porous materials regime [27–29]. Built from sensitive organic ligands and a wide range of metal ion/clusters, these materials outperform their contemporaries due to their large surface area, structural tunability of the pore metrics, functional nano-spaces [30]. MOFs have received a lot of attention in the scientific community as fluorometric sensors for detecting a lot of analytes [31].

Luminescent MOF (LMOFs) have so gained interest due to their improved guest identification capabilities and subsequent analyte specific optical response. The sensing mechanism may be divided into two categories based on the electrical nature of the analyte and/or MOFs: *a)* "turn-off" and *b)* "turn-on" sensing. In general, a turn-on response may be elicited by constraining non-radiative relaxations in MOFs via *a)* integration of stiff functional groups, *b)* or exciplex/excimer production with incoming guest molecules, and so on. Thus, contemporary research efforts are directed towards the creation of appropriate sensors capable of eliciting a turn-on response based on LMOFs. Aromatic conjugated organic linkers have been discovered to be particularly important for the emission property of LMOFs in the majority of situations. Light is absorbed by π-rich conjugated linkers, and the subsequent radiative transition of this energy results in the luminescence characteristic of LMOFs. Apart from ligand-based luminescence, charge transfer mechanisms involving aromatic organic linkers (inter-ligand charge transfer (ILCT), metal–ligand charge transfer (MLCT), ligand–metal charge transfer (LMCT), etc.) have also been reported. Such ligand-based luminescence in LMOFs has demonstrated enormous potential for the fabrication of sensory materials [32].

Microcrystalline cellulose (MCC) modified MOFs offer several advantages over their traditional inorganic counterparts. The incorporation of MCC into MOFs results in a material with high surface area, providing an increased number of active sites available for interaction. As a result, MCC-MOFs have demonstrated enhanced efficiency in various extraction applications [33–35]. Furthermore, the use of MCC as a raw material is advantageous due to its renewable and sustainable nature, being derived from plant-based sources. Additionally, the cost-effectiveness of MCC as compared to other materials commonly used in MOFs adds to its appeal for large-scale production. Finally, MCC's biodegradability makes it more environmentally friendly than traditional MOFs which often contain non-biodegradable components.

In this work, Ca-BTC/MCC MOF hybrid was prepared and applied for the selective detection of MSG in instant noodles seasonings. To the best of our knowledge, this work is the report of using Ca-BTC/MCC MOF as a fluorescent sensor. Compared with the other reported methods of MSG determination, this spectrofluorometric method is rapid, reliable, selective and environmentally friendly which make it suitable for the routine analysis of MSG in food and food derived products. To the best of our knowledge, this work reports for the first time the application of Ca-BTC/MCC MOF composite as a sensitive sensor for spectrofluorometric detection. Compared with Ca-BTC MOF, the composite has higher surface area which offers higher sensitivity for the determination of MSG. Moreover, the prepared composite is biodegradable, stable, eco-friendly, and efficient nanoprobe.

2. Experimental

2.1. Instrumentation

All fluorescence spectra measurements were recorded using a Jasco model FP-8300 spectrofluorometer (Tokyo, Japan) equipped with a 1-cm quartz cuvette, both excitation and emission bandwidths were set at 10 nm. The excitation wavelength was set at 325 nm while the emission wavelength was set at 422 nm. The software of Spectra Manager (Jasco Co., Tokyo, Japan) was used for spectral data processing and acquisition. Jenway® 3510 pH-meter (Staffordshire,UK) was also employed for phase pH adjustment. BET measurements were carried out using Autosorb-01 (Quantachrome TouchWin™). To analyze the morphological characteristics of MOFs, SEM images were collected

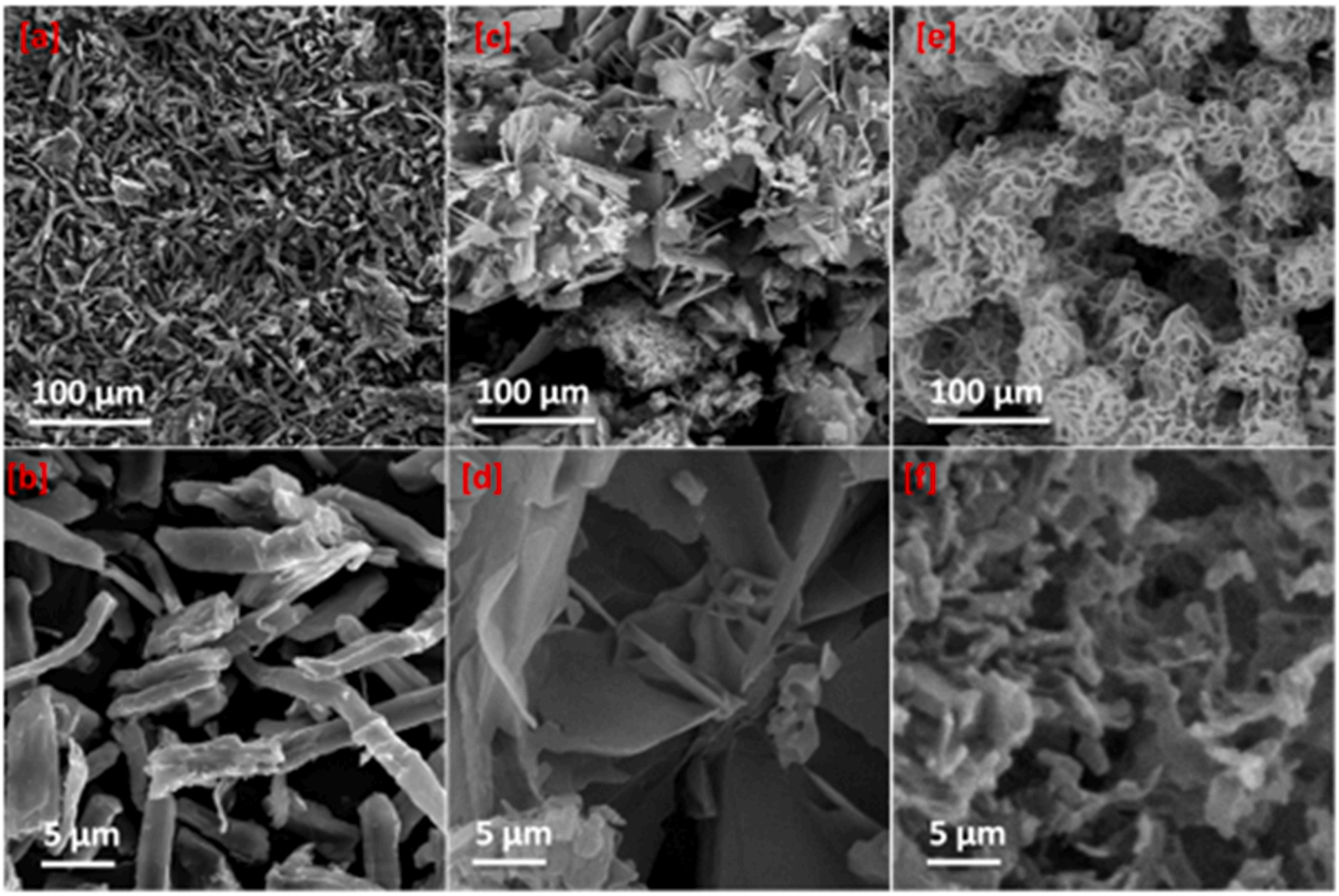

Fig. 3. SEM images of [a,b] the MCC polymer, [c,d] the Ca-BTC MOF, and [e,f] the Ca-BTC/MCC MOF hybrid.

using an HRSEM Quanta FEG 250 with field emission gun. To characterize the crystallinity and phase purity of the produced MOFs, a Malvern Panalytical X'PertPRO PANalytical diffractometer (K X-ray at 45 kV, 40 mA, = 1.5406) was utilised. A JASCO FT/IR 6100 spectrometer was used to analyze the Fourier transforms infrared spectra of MOFs.

2.2. Materials

Monosodium glutamate (99 %) was kindly supplied from by Sigma Pharmaceutical Industries (Quesna, El-Menoufia, Egypt). Methanol, ethanol and acetonitrile, $CaCl_2$, 1,3,5-benzenetricarboxylic acid (BTC), sodium hydroxide, and microcrystalline cellulose were purchased from Merck (Darmstadt, Germany).

2.3. Synthesis of Ca-BTC/MCC MOF

Ca-BTC was prepared, as reported [28] by using the following conditions: 1,3,5-benzenetricarboxylic acid (0.42 g) was dissolved in 100 mL of 1 M NaOH solution. In parallel, $CaCl_2$ (0.316 g) was dissolved in 10 mL of purified water. At 25 °C, the two solutions were combined and agitated for 20 min. The reaction mixture was maintained at 90 °C for 24 hrs in the oven. Following this time, Ca-BTC was collected, washed with 99.9 % ethanol, and then passed through a Whatmann filter paper.

Ca-BTC/MCC MOF composites was prepared under the same conditions in the synthesis of Ca-BTC MOF as follows [28]: MCC (0.5 g) and of 1,3,5-benzenetricarboxylic acid (0.42 g) were dissolved in 100 mL of 1 M NaOH solution and water soluble $CaCl_2$ (0.316 g) was added dropwise to the mixture of MCC/BTC at 25 °C while shaken the solution for 20 min. Then, the mixture was added in dry oven at 90 °C for 24 hrs. The white solids were formed in the bottom of the vessel. Following a centrifugation of the mixture, two ethanol washes, and a 12-hour vacuum drying process at 60 °C, the composites were obtained and stored until used.

2.4. Procedures for determination of MSG

An amount of 5 mg/mL of Ca-BTC-MCC stock were prepared by addition of 500 mg of Ca-BTC/MCC composite in 100 volumetric flask, the volume was completed to 100 mL by deionized water. The system was sonicated for 30 min to enhance dispersion of the composite. Finally, the dispersion system was filtrated by 0.22 µm syringe filter. For MSG detection, 125 µL of Ca-BTC-MCC system was added to 25 mL of MSG aqueous solution and the mixture was measured immediately at 422 nm after excitation at the wavelength of 325 nm.

2.5. Measurement of quantum yield

The QY of the Ca-BTC/MCC MOF was detected using the single-point method (Eq.1):

$$QY = QY_{QS} \times (F_{Ca-BTC/MCC}/F_{QS} \times (A_{QS}/A_{Ca-BTC/MCC}) \times \left(\eta_{Ca-BTC/MCC}/\eta_{QS}\right)^2$$

Where F is the integrated fluorescence intensity, A is the absorbance and η is the refractive index of the solvent. Quinine sulfate (QS) was used as the standard. QS was dissolved in 0.1 M sulfuric acid.The absorbance value was set at 0.05 to standardize the absorbance impact. In an aqueous solution, the ηCQD/ ηQS = 1.

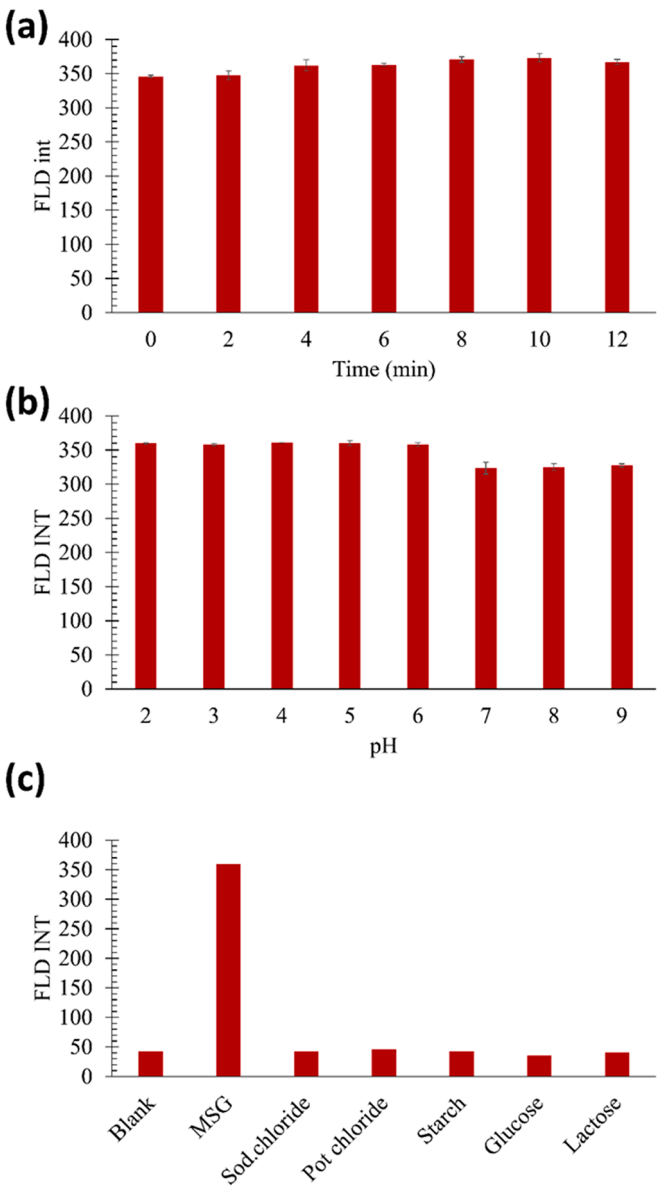

Fig. 4. The effect of incubation time (a), pH (b) and interferences (c) on the fluorescence intensity using water as a disperser solvent, 125 μL of Ca-BTC/MCC, 25 mL of MSG aqueous solution.

2.6. Method validation

The proposed method was validated according to International Guidelines ICH Q2(R2) [36] in terms of selectivity, linearity, limit of quantitation, and accuracy (trueness and precision).

3. Results and discussion

3.1. Characterization of Ca-BTC/MCC MOF

The structures of Ca-BTC and MCC experienced alterations during the synthesis of the Ca-BTC/MCC MOF composite sorbent, and these changes in chemical bonds and interactions were studied by FTIR. Fig. 1**a** displays MCC's FTIR spectrum. The band at 1024 cm^{-1} was assigned to C-O, whereas the CH_2-CH group emerged at 2900 cm^{-1}, and the O-H group appeared at 3347 cm^{-1}. The O-H expansion over hydrogen bonding with water and CaO was illustrated by the peaks at 3306 cm^{-1}, 1149 cm^{-1}, and 1021 cm^{-1}, respectively, as shown in the Ca-BTC FT-IR spectrum (Fig. 1**b**). At 1632.01 cm^{-1}, one may observe the isotope of the bending mode of unbound water. The region of 1700 to 1300 cm^{-1} is where asymmetric and symmetric O-C-O stretching of the carboxyl groups occur. Asymmetric O-C-O stretching is linked to the peaks at 1574.50 cm^{-1}, 1556 cm^{-1}, and 1510 cm^{-1}, whereas symmetric O-C-O stretching is responsible for the peaks at 1435.50 cm^{-1} and 1392 cm^{-1}. The FTIR spectrum interaction between Ca-BTC and MCC is presented in Fig. 1**c**. These results indicated that the composite showed distinct Ca-BTC uptake bands in addition to the MCC uptake bands.

The crystallinity of the prepared hybrid was studied and compared with MCC and Ca-BTC MOF using PXRD. Fig. 2**a** reports the diffraction pattern of MCC. The MCC crystal structures showed the large peaks at 12.10°, 20.10°, 22.30°, and 34.60°, which were characteristic for cellulose II crystals. The Ca-BTC diffraction pattern is seen in Fig. 2**b**. The PXRD peaks have the following unit cell parameters: a = 10.94, b = 6.73, c = 18.58, and α = β = γ = 90.00° (orthorhombic). Space group Pnm a 63 has been used to index the PXRD peaks. The Ca-BTC/MCC diffraction patterns are shown in Fig. 2**c**. The compounds exhibited distinct Ca-BTC diffraction bands, suggesting that MCC has been effectively integrated into the crystalline Ca-BTC production process.

For the sake of comparison, the morphology of MCC was examined. As seen in the SEM pictures in Fig. 3**a and b**, the 3D lattice structure with uniformly dispersed particles and massive particle agglomerations was clearly visible. The FE-SEM images displayed in Fig. 3**c and d** depicted the typical crystal structure of Ca-BTC. Using an electron microscope, the morphological properties of the Ca-BTC/MCC MOF were investigated and the findings displayed in Fig. 3**e and f**. Measured under a microscope, the crystal size of the hybrid material was two-dimensional, with one side measuring 2.20 μm and the other side measuring 12.10 μm. The fact that the composite shape's characteristics were entirely distinct from those of MCC and Ca-BTC indicates that both compounds were successfully encapsulated. The measured BET surface areas from N_2 adsorption–desorption for MCC, Ca-BTC, and Ca-BTC/MCC were 10.60, 560.00, and 820.00 m^2 g^{-1}, respectively. Fig. S1 shows an overlay of the excitation and emission spectra of Ca-BTC/MCC MOF. The stability the MOF composite was assessed on short- and long-term basis. The Ca-BTC/MCC MOF was found stable in benchtop study over 24 h, and the in the fridge at −4°C for seven days. The prepared Ca-BTC/MCC MOF was stored in solid form at room temperature, and its fluorescence intensity remained stable with no significant changes observed over a period of 6 months.

3.2. Method optimization

Studying the different experimental variables that may affect the method performance is crucial. The one-variable-at-a-time (OVAT) approach was used in the optimization process. Different factors were investigated, including excitation wavelength, disperser solvent of MOF, incubation time, and pH of the aqueous sample. Fluorescence intensity was monitored at each condition to reach the maximum sensitivity.

3.2.1. Excitation wavelength optimization

Changing the excitation wavelength can greatly influence the emission intensity in fluorescence spectroscopy. The impact of excitation wavelength on the intensity of Ca-BTC/MCC MOF was examined across the range 225–350. As reported in *Supplementary materials section S.1*, the highest emission was observed at 422 nm with an excitation wavelength of 325 nm. This specific excitation wavelength was utilized in subsequent steps to determine the concentration of MSG in both aqueous solutions and instant noodles seasonings.

3.2.2. Effect of disperser solvent of MOF

Different solvents were used for dispersion of Ca-BTC/MCC MOF composite including methanol, ethanol, acetonitrile and deionized water. A concentration of 5 mg/mL of Ca-BTC/MCC MOF composite was prepared in different solvents, and then the dispersion system was

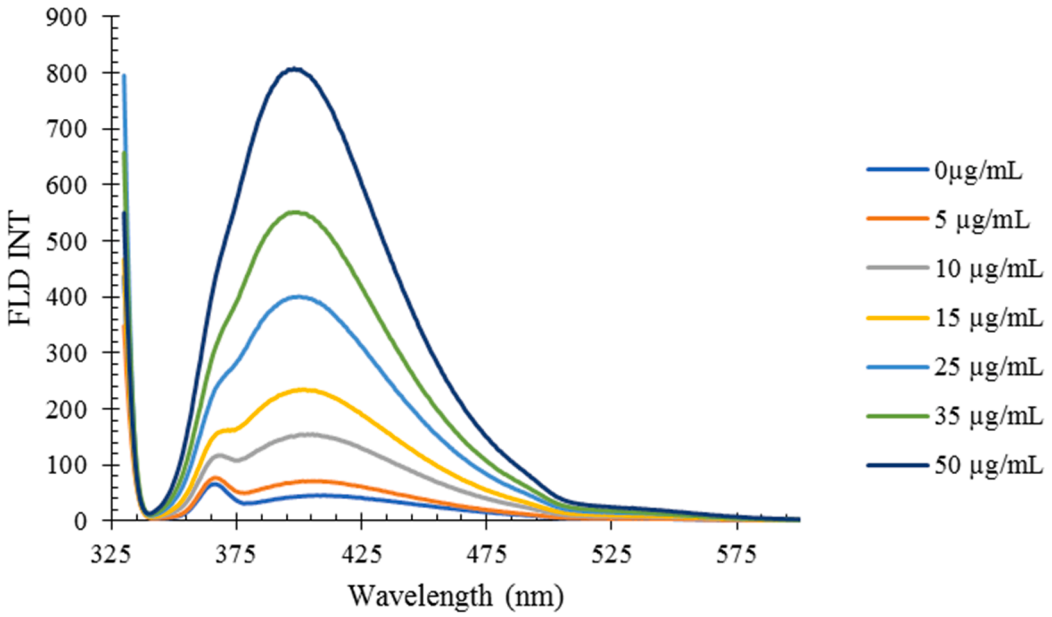

Fig. 5. Overlaid spectra of different concentrations of MSG over the studied linearity range.

Table 1
Intra-day and inter-day precision and trueness.

	Intraday			Interday		
	Added (µg/mL)	Found (µg/mL)	Found (%) ±RSD	Added (µg/mL)	Found (µg/mL)	Found (%) ±RSD
MSG	8	8.1	100.8 ± 0.1	8	8.0	100.4 ± 0.5
	30	30.2	100.6 ± 0.1	30	30.0	100.0 ± 0.8
	45	45.7	101.5 ± 0.4	45	45.2	100.4 ± 0.9
Mean			100.96			100.3
RSD (%)			0.2			0.7

Table 2
Application of the developed method for determination of MSG in food sample using standard addition method.

	Added (µg/mL)	Found (µg/mL)	Found (%)
MSG	5	5.0	100.5
	5	4.9	98.1
	5	5.1	100.9
	5	5.1	101.5
	5	4.9	99.5
	5	4.9	98.6
Mean			99.9
%RSD			1.4

sonicated for 30 min followed by filtration using a syringe filter (0.22 µm). Only water achieved fluorescence intensity while the other organic solvents achieved negligible fluorescence intensity. It could be attributed to the low tendency of organic solvents to achieve a good dispersion MOF hybrid.

3.2.3. *Effect of incubation time*

Different incubation times were investigated in the range from 0 to 12 min as indicated in Fig. 4**a**. There was no significant change in FLD intensity over time. This is because the interaction between MSG and the Ca-BTC/MCC MOF hybrid is instantaneous, which allows for the rapid measurement of MSG and makes the developed method time-saving besides being less-laborious than other derivatization-based methods.

3.2.4. *Effect of pH on MOF emission*

Different pH values were investigated over the range 2 to 9. As indicated in Fig. 4**b**, there was no significant change with pH variations over the studied range. This could be explained by the high stability of Ca-BTC/MCC MOF and the negligible effect of pH on the predominately charged amine group in MSG at pH values $\leq$ 9. Accordingly, deionized water was used as diluent throughout the following procedure. The calculated quantum yield of Ca-BTC/MCC MOF was found to be 3.8 % at an excitation wavelength of 325 nm, and an emission wavelength of 422 nm.

3.3. *Method validation*

3.3.1. *Selectivity*

Selectivity of analytical methods is a key parameter during method development. The method is deemed selective if there is no interference from interfering substances, according to ICH guidelines. The reaction was examined in the presence of chemicals that may be present as a contemporaneous component with MSG in food preparations to determine the method's selectivity such as glucose, lactose, sodium chloride, potassium chloride, and starch. No significant changes were observed in the fluorescence intensity, using saturated solutions of theses food ingredients, which indicated the adequate method selectivity for MSG, as shown in Fig. 4**c**.

3.3.2. *Linearity, range and limit of quantitation*

To investigate the linearity of the method, a calibration curve was constructed by plotting the FLD intensity on the y-axis and the concentration of MSG (in µg/mL) on the x-axis. The calibration curve indicated that the technique exhibited linearity within the 5–50 µg/mL MSG concentration range (Fig. 5). The calculated coefficient of determination (r^2) was 0.9993. The limit of quantitation was found to be 5 µg/mL, demonstrating the high applicability of the proposed method in food analysis. The constructed calibration curve is shown in Fig. S2.

3.3.3. *Accuracy (precision and trueness)*

The accuracy of the method was evaluated by analyzing three quality

Table 3
Comparison between the developed method and other reported methods for MSG determination in different food matrices.

Sample	Analytical technique	Nanoparticles	Analysis time	LOQ	Solvent	Ref.
Vegetable soup	Electrochemical	Gold nanoparticles decorated on molybdenum disulfide chitosan	1 hr	0.1 μM	Ethanol	[37]
Tomato soup	Electrochemical	Montmorillonite decorated poly caprolactone and chitosan based nanofibers	1 hr	5.42 μM	Formic acid, acetone	[38]
Mandarin fish	Electrochemical	Gold nanoparticles	24 hr	Not reported	Acetic acid	[39]
Vegetable soup	Electrochemical	Platinum nanoparticles	24 hr	1.59 μM	Acetic acid and methanol	[40]
Instant noodles, chicken cubes	Spectroflourimetry	Carbon quantum dots	1.5 min	66 μM	Water	[41]
Instant noodles	Spectroflourimetry	Ca-BTC/MCC MOF	1 min	5 μg/mL	Water	This work

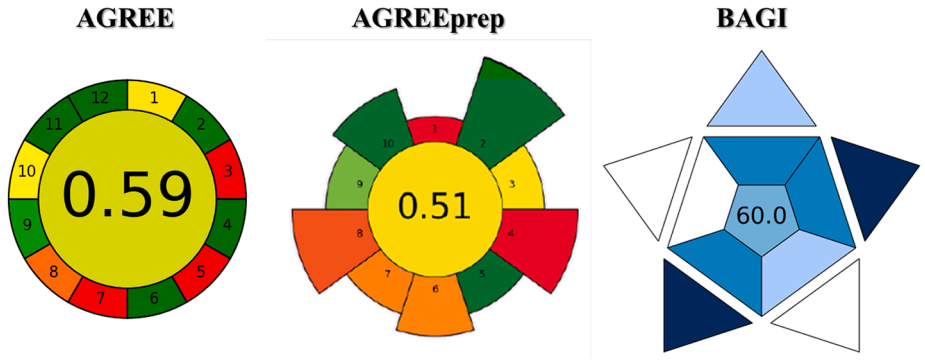

Fig. 6. Pictograms related to AGREE, AGREEprep, and BAGI evaluation of the proposed procedure.

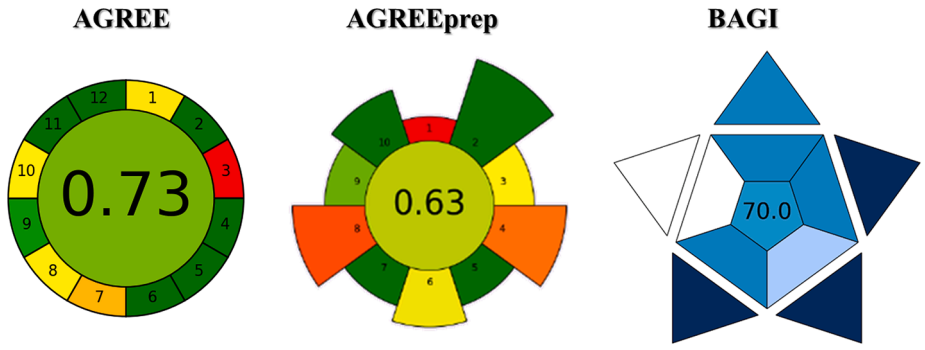

Fig. 7. Pictograms related to AGREE, AGREEprep, and BAGI re-evaluation of the proposed procedure following some improvements.

control samples spiked with MSG at three different concentrations (8, 30, and 45 μg/mL). MSG concentrations were analyzed in triplicate. Table 1 shows that the procedure trueness (given in terms of recovery %) was adequate for the application of the proposed method on food sample. The recoveries (%) were found in the range of 100.0 to 101.5 and the %RSDs were in the range of 0.1 to 0.9 %. Accordingly, the developed nanoprobe spectrofluorimetric analytical method is accurate according to ICH (Q2)R2 guidelines.

4. Application on food sample

The developed nanoprobe spectrofluorometric method was utilized for the determination of MSG from a single packet of instant noodles containing a sachet of seasoning powder. Since the application was performed on seasoning powder, no extensive sample preparation was required. 100 mg of the powder was diluted to 100 mL, and then the mixture was sonicated for 20 min. Subsequently, the solution was filtered through a 0.22 μm syringe filter. A 1000 μL aliquot from the previous system was further diluted to 25 mL, and 125 μL of Ca-BTC/MCC MOF was added to this solution. These procedures resulted in a concentration of 20.15 μg/mL.

Standard addition was employed to assess the matrix effect; specifically, 5 μg/mL of MSG was added to the previous system, and six replicates were performed. As shown in Table 2, the percent recovery fell within the range of 98.1 % to 101.5 %, with a percent relative standard deviation (RSD%) of 1.4 %. These results indicated that the developed method can been successfully applied for the determination of MSG in food samples. Table 3 compares between the developed method and other recent methods for MSG determination in different food matrices.

5. Green profile evaluation

The developed nanoprobe spectrofluorometric method was further evaluated in terms of green profile by means of the recent accepted tools [42] like AGREE (Analytical GREEnness Metric Approach) [43], AGREEprep (Analytical greenness metric for sample preparation) [44], and BAGI (Blue applicability grade index) [45].

As highlighted in Fig. 6, based on the metrics currently accepted for

the evaluation of the green profile, the method reported here certainly shows a reduced environmental impact both on the basis of the AGREE (criteria 2, 4, 6, 9, 11 and 12), and based on AGREEprep (criteria 2, 5, 9 and 10). Based on the score obtained from BAGI, can be stated that the method can be considered "practical" (score of 60). The specific inputs used are reported in *Supplementary materials section S3*.

Certainly, the procedure could be improved compared to the procedure reported here with a view to obtaining an even greener profile and a higher BAGI score. In particular, if the procedure is improved by using a sample preparator (automated) which also increases the number of samples that can be processed (approx. 10 samples/h) and by reducing the quantity of sample (10 mg) and proportionally the quantity of waste (12.5 mL) can see in Fig. 7 how the green and BAGI profiles improves significantly. The specific inputs used are reported in *Supplementary materials section S.4*.

6. Conclusions

A novel turn-on spectrofluorometric method has been developed for the determination of MSG in food samples with acceptable accuracy and precision. MOFs, composed of metal ions/clusters and organic ligands, offer versatile applications due to their inherent crystallinity, distinct structure, adjustable porosity, and diverse functionalization. The structural and chemical adaptability of MOFs allows for high selectivity through pore-sieving mechanisms, making LMOFs a notable choice as sensing materials in recent times. By leveraging their high internal surface areas, MOFs can concentrate analytes effectively, leading to lower detection limits and enhanced sensitivity.

This study presents the synthesis and characterization of a reusable, biodegradable, stable, eco-friendly, and efficient nanoprobe sensor for MSG detection using the Ca-BTC/MCC MOF hybrid. The ligand-based luminescent sensor was thoroughly characterized using FTIR, HR-SEM, and PXRD techniques. The developed nanoprobe spectrofluorimetric approach enables the selective determination of MSG in food samples with good sensitivity. The method offers a quick, cost-effective procedure with high recovery rates, rendering it a valuable asset for MSG detection in food samples.

Notably, the proposed method demonstrates excellent selectivity in identifying MSG in instant noodles' seasonings, achieving good linearity, and accuracy (precision and trueness), in line with the ICH Q2(R2) guidelines, but also showing an interesting reduced environmental impact following the metrics currently accepted for the evaluation of the green profile and practicability.

CRediT authorship contribution statement

Alaa Bedair: Writing – original draft, Investigation, Formal analysis, Data curation, Conceptualization. **Reda Abdelhameed:** Writing – original draft, Methodology, Investigation, Formal analysis, Data curation, Conceptualization. **Sherin F. Hammad:** Supervision, Project administration, Methodology, Formal analysis, Conceptualization. **Inas A. Abdallah:** Supervision, Project administration, Methodology, Formal analysis, Conceptualization. **Marcello Locatelli:** Writing – original draft, Methodology, Formal analysis, Conceptualization. **Fotouh R. Mansour:** Writing – original draft, Supervision, Project administration, Methodology, Formal analysis, Conceptualization.

Declaration of competing interest

The authors declare that they have no known competing financial interests or personal relationships that could have appeared to influence the work reported in this paper.

Data availability

Data will be made available on request.

Appendix A. Supplementary data

Supplementary data to this article can be found online at https://doi.org/10.1016/j.microc.2024.111132.

References

[1] F. Bellisle, Glutamate and the UMAMI taste: sensory, metabolic, nutritional and behavioural considerations. A review of the literature published in the last 10 years, Neurosci. Biobehav. Rev. 23 (1999) 423–438, https://doi.org/10.1016/S0149-7634(98)00043-8.

[2] D. Çelik Ertuğrul, FoodWiki: a Mobile App Examines Side Effects of Food Additives Via Semantic Web, J. Med. Syst. 40 (2016) 41, https://doi.org/10.1007/s10916-015-0372-6.

[3] C.B. Quines, S.G. Rosa, J.T. Da Rocha, B.M. Gai, C.F. Bortolatto, M.M.M.F. Duarte, C.W. Nogueira, Monosodium glutamate, a food additive, induces depressive-like and anxiogenic-like behaviors in young Rats, Life Sci. 107 (2014) 27–31, https://doi.org/10.1016/j.lfs.2014.04.032.

[4] M. Soyseven, H.Y. Aboul-Enein, G. Arli, Development of a HPLC method combined with ultraviolet/diode array detection for determination of monosodium glutamate in various food samples, Int. J. Food Sci. Technol. 56 (2021) 461–467, https://doi.org/10.1111/ijfs.14661.

[5] T. Populin, S. Moret, S. Truant, L.S. Conte, A survey on the presence of free glutamic acid in foodstuffs, with and without added monosodium glutamate, Food Chem. 104 (2007) 1712–1717, https://doi.org/10.1016/j.foodchem.2007.03.034.

[6] A. Zanfirescu, A. Ungurianu, A.M. Tsatsakis, G.M. Nițulescu, D. Kouretas, A. Veskoukis, D. Tsoukalas, A.B. Engin, M. Aschner, D. Margină, A Review of the Alleged Health Hazards of Monosodium Glutamate, Compr. Rev. Food Sci. Food Saf. 18 (2019), https://doi.org/10.1111/1541-4337.12448.

[7] C.C. Acebal, A.G. Lista, B.S. Fernández Band, Simultaneous determination of flavor enhancers in stock cube samples by using spectrophotometric data and multivariate calibration, Food Chem. 106 (2008) 811–815, https://doi.org/10.1016/j.foodchem.2007.06.009.

[8] T.N. Olivares-Bañuelos, I. Martínez-Hernández, L.C. Hernández-Kelly, D. Chi-Castañeda, L. Vega, A. Ortega, The neurotoxin diethyl dithiophosphate impairs glutamate transport in cultured Bergmann glia cells, Neurochem. Int. 123 (2019) 77–84, https://doi.org/10.1016/j.neuint.2018.06.004.

[9] D.D. Baciu, A. Matei, T. Visan, Extraction procedure and cyclic voltammetry assay for detection of monosodium glutamate from different processed food sources, Rev. Chim. 71 (2020) 63–71. https://doi.org/10.37358/RC.20.8.8279.

[10] M. Shannon, B. Green, G. Willars, J. Wilson, N. Matthews, J. Lamb, A. Gillespie, L. Connolly, The endocrine disrupting potential of monosodium glutamate (MSG) on secretion of the glucagon-like peptide-1 (GLP-1) gut hormone and GLP-1 receptor interaction, Toxicol. Lett. 265 (2017) 97–105, https://doi.org/10.1016/j.toxlet.2016.11.015.

[11] H.M. Ali, S.F. Hammad, S.F. El-Malla, Green spectrophotometric methods for determination of a monosodium glutamate in different matrices, Microchem. J. 169 (2021) 106622, https://doi.org/10.1016/j.microc.2021.106622.

[12] A. Afraa, A. Mounir, A. Zaid, Colorimetric Determination of Monosodium Glutamate in Food Samples Using Colorimetric Determination of Monosodium Glutamate in Food Samples Using L-glutamate Oxidase-glutamate Oxidase, Chinese J. Appplied Environ. Biol. 19 (2013) 1069, https://doi.org/10.3724/SP.J.1145.2013.01069.

[13] W. Khampha, V. Meevootisom, S. Wiyakrutta, Spectrophotometric enzymatic cycling method using l-glutamate dehydrogenase and d-phenylglycine aminotransferase for determination of l-glutamate in foods, Anal. Chim. Acta. 520 (2004) 133–139, https://doi.org/10.1016/j.aca.2004.05.044.

[14] D. Marlina, A. Amran, A. Ulianas, Monosodium Glutamate Analysis in Meatballs Soup, IOP Conf. Ser. Mater. Sci. Eng. 335 (2018) 012033, https://doi.org/10.1088/1757-899X/335/1/012033.

[15] E. Valero, F. Garcia-Carmona, A Continuous Spectrophotometric Method Based on Enzymatic Cycling for Determiningl-Glutamate, Anal. Biochem. 259 (1998) 265–271, https://doi.org/10.1006/abio.1998.2650.

[16] W. Nasomphan, P. Tangboriboonrat, S. Tanapongpipat, S. Smanmoo, Selective fluorescent detection of aspartic acid and glutamic acid employing dansyl hydrazine dextran conjugate, J. Fluoresc. 24 (2014) 7–11, https://doi.org/10.1007/s10895-013-1269-8.

[17] F.G. Sánchez, A.A. Gallardo, Liquid chromatographic and spectrofluorimetric determination of aspartame and glutamate in foodstuffs following fluorescamine fluorigenic labelling, Anal. Chim. Acta. 270 (1992) 45–53, https://doi.org/10.1016/0003-2670(92)80090-T.

[18] A. Sharma, N.S.M. Quantrill, Novel L-glutamate assay based on fluorescence quenching, Biomed. Fiber Opt. Instrum. 2131 (1994) 591, https://doi.org/10.1117/12.180765.

[19] N. Veni, D. Karthika, M. Surya Devi, M.F. Rubini, M. Vishalini, Y.J. Pradeepa, Analysis of monosodium l-glutamate in food products by high-performance thin layer chromatography, J. Young Pharm. 2 (2010) 297–300, https://doi.org/10.4103/0975-1483.66795.

[20] D.H. Daniels, F.L. Joe, G.W. Diachenko, Determination of free glutamic acid in a variety of foods by high-performance liquid chromatography, Food Addit. Contam. 12 (1995) 21–29, https://doi.org/10.1080/02652039509374275.

[21] A.T. Rhys Williams, S.A. Winfield, Determination of monosodium glutamate in food using high-performance liquid chromatography and fluorescence detection, Analyst 107 (1982) 1092–1094, https://doi.org/10.1039/AN9820701092.

[22] C.F. Saller, M.J. Czupryna, γ-Aminobutyric acid, glutamate, glycine and taurine analysis using reversed-phase high-performance liquid chromatography and ultraviolet detection of dansyl chloride derivatives, J. Chromatogr. B Biomed. Sci. Appl. 487 (1989) 167–172, https://doi.org/10.1016/S0378-4347(00)83020-0.
[23] D.D. Baciu, A. Matei, A. Cojocaru, T. Visan, Electrochemical impedance spectroscopy in nitrate solutions containing monosodium glutamate using screen-printed electrodes, UPB Sci, Bull. Ser. B Chem. Mater. Sci. 82 (2020) 47–62.
[24] R. Devi, S. Gogoi, S. Barua, H. Sankar Dutta, M. Bordoloi, R. Khan, Electrochemical detection of monosodium glutamate in foodstuffs based on Au@MoS 2 /chitosan modified glassy carbon electrode, Food Chem. 276 (2019) 350–357, https://doi.org/10.1016/j.foodchem.2018.10.024.
[25] H.P. Aung, U. Pyell, In-capillary derivatization with o-phthalaldehyde in the presence of 3-mercaptopropionic acid for the simultaneous determination of monosodium glutamate, benzoic acid, and sorbic acid in food samples via capillary electrophoresis with ultraviolet detectio, J. Chromatogr. a. 1449 (2016) 156–165, https://doi.org/10.1016/j.chroma.2016.04.033.
[26] R.H. Elattar, A.H. Kamal, F.R. Mansour, S.F. El-Malla, Spectrophotometric determination of monosodium glutamate in instant noodles' seasonings and Chinese salt by ligand exchange complexation, J. Food Compos. Anal. 121 (2023) 105404, https://doi.org/10.1016/j.jfca.2023.105404.
[27] L.E. Kreno, K. Leong, O.K. Farha, M. Allendorf, R.P. Van Duyne, J.T. Hupp, Metal-Organic Framework Materials as Chemical Sensors, Chem. Rev. 112 (2012) 1105–1125, https://doi.org/10.1021/cr200324t.
[28] R.M. Abdelhameed, S.F. Hammad, I.A. Abdallah, A. Bedair, M. Locatelli, F. R. Mansour, A hybrid microcrystalline cellulose/metal-organic framework for dispersive solid phase microextraction of selected pharmaceuticals: A proof-of-concept, J. Pharm. Biomed. Anal. 235 (2023) 115609, https://doi.org/10.1016/j.jpba.2023.115609.
[29] S.F. Hammad, I.A. Abdallah, A. Bedair, R.M. Abdelhameed, M. Locatelli, F. R. Mansour, Metal organic framework-derived carbon nanomaterials and MOF hybrids for chemical sensing, TrAC, Trends Anal. Chem. (2024) 117425, https://doi.org/10.1016/j.trac.2023.117425.
[30] F.R. Mansour, S.F. Hammad, I.A. Abdallah, A. Bedair, R.M. Abdelhameed, M. Locatelli, Applications of metal organic frameworks in point of care testing, TrAC Trends Anal. Chem. 172 (2024) 117596, https://doi.org/10.1016/j.trac.2024.117596.
[31] F.R. Mansour, R.M. Abdelhameed, S.F. Hammad, I.A. Abdallah, A. Bedair, M. Locatelli, A Microcrystalline Cellulose/Metal-Organic Framework Hybrid for Enhanced Ritonavir dispersive solid phase microextraction from Human Plasma, Carbohydr. Polym. Technol. Appl 7 (2024) 100453, https://doi.org/10.1016/j.carpta.2024.100453.
[32] S. Furukawa, J. Reboul, S. Diring, K. Sumida, S. Kitagawa, Structuring of metal-organic frameworks at the mesoscopic/macroscopic scale, Chem. Soc. Rev. 43 (2014) 5700–5734, https://doi.org/10.1039/c4cs00106k.
[33] B. Joarder, A.V. Desai, P. Samanta, S. Mukherjee, S.K. Ghosh, Selective and sensitive aqueous-phase detection of 2,4,6-trinitrophenol (TNP) by an amine-functionalized metal-organic framework, Chem. - A Eur. J. 21 (2015) 965–969, https://doi.org/10.1002/chem.201405167.
[34] A. Karmakar, P. Samanta, S. Dutta, S.K. Ghosh, Fluorescent "Turn-on" Sensing Based on Metal – Organic Frameworks (MOFs), Chem. an Asian J. (2019) 4506–4519, https://doi.org/10.1002/asia.201901168.
[35] F. Ghaemi, A. Amiri, Microcrystalline cellulose/metal−organic framework hybrid as a sorbent for dispersive micro-solid phase extraction of chlorophenols in water samples, J. Chromatogr. a. 1626 (2020) 461386, https://doi.org/10.1016/j.chroma.2020.461386.
[36] ICH Q2(R2) Validation of Analytical Procedures, Guidance for Industry. March 2024 ICH-Quality Revision 2. https://www.fda.gov/regulatory-information/search-fda-guidance-documents/q2r2-validation-analytical-procedures.
[37] R. Devi, S. Gogoi, S. Barua, H. Sankar Dutta, M. Bordoloi, R. Khan, Electrochemical detection of monosodium glutamate in foodstuffs based on Au@MoS2/chitosan modified glassy carbon electrode, Food Chem. 276 (2019) 350–357, https://doi.org/10.1016/j.foodchem.2018.10.024.
[38] H. Atilgan, B. Unal, E.E. Yalcinkaya, G. Evren, G. Atik, F. Ozturk Kirbay, N.M. Kilic, D. Odaci, Development of an Enzymatic Biosensor Using Glutamate Oxidase on Organic–Inorganic-Structured, Electrospun Nanofiber-Modified Electrodes for Monosodium Glutamate Detection, Biosensors 13 (2023) 430, https://doi.org/10.3390/bios13040430.
[39] Y. Wang, L. Kong, G. Shu, G. Sun, Y. Feng, M. Zhu, Development of sensitive and stable electrochemical impedimetric biosensor based on T1R1 receptor and its application to detection of umami substances, Food Chem. 423 (2023) 136233, https://doi.org/10.1016/j.foodchem.2023.136233.
[40] J. Liu, Y. Fan, G. Chen, Y. Liu, Highly sensitive glutamate biosensor based on platinum nanoparticles decorated MXene-Ti3C2Tx for l-glutamate determination in foodstuffs, LWT. 148 (2021) 111748, https://doi.org/10.1016/j.lwt.2021.111748.
[41] F.R. Mansour, M.A.A. Hamid, A. Gamal, S.H. Elagamy, Nitrogen sulfur co doped carbon quantum dots as fluorescent probe for quantitative determination of monosodium glutamate in food samples, J. Food Compos. Anal. 127 (2024), https://doi.org/10.1016/j.jfca.2024.105972.
[42] M. Locatelli, A. Kabir, M. Perrucci, S. Ulusoy, H.I. Ulusoy, I. Ali, Green profile tools: current status and future perspectives, Advances in Sample Preparation 6 (2023) 100068, https://doi.org/10.1016/j.sampre.2023.100068.
[43] F. Pena-Pereira, W. Wojnowski, M. Tobiszewski, AGREE—Analytical GREEnness Metric Approach and Software, Anal. Chem. 92 (2020) 10076–10082, https://doi.org/10.1021/acs.analchem.0c01887.
[44] W. Wojnowski, M. Tobiszewski, F. Pena-Pereira, E. Psillakis, AGREEprep – Analytical greenness metric for sample preparation, TrAC Trends Anal. Chem. 149 (2022) 116553, https://doi.org/10.1016/j.trac.2022.116553.
[45] N. Manousi, W. Wojnowski, J. Płotka-Wasylka, V. Samanidou, Blue applicability grade index (BAGI) and software: a new tool for the evaluation of method practicality, Green Chem. 25 (2023) 7598–7604, https://doi.org/10.1039/D3GC02347H.